CFD Letters

Journal homepage:
https://semarakilmu.com.my/journals/index.php/CFD_Letters/index
ISSN: 2180-1363

Investigation of Vertical Axis Wind Turbine Performance with Savonius Rotor on Air Ejector Dimensions using Computational Fluid Dynamics

Ismail[1], Rinawati[1], Imam Muzaki[1,2,*]

[1] Department of Mechanical Engineering, Faculty of Engineering, Universitas Pancasila, Srengseng Sawah. Jagakarsa 12640, DKI Jakarta, Indonesia
[2] Department of Mechanical Engineering, Faculty of Engineering, Universitas Buana Perjuangan Karwang, Karawang, 41361, Jawa Barat, Indonesia

ARTICLE INFO

Article history:
Received 25 June 2023
Received in revised form 21 July 2023
Accepted 19 August 2023
Available online 10 January 2024

Keywords:
Tsunami Bore Forces; Froude Number; Land Structure; CFD; inundation depth

ABSTRACT

This study evaluates the tsunami forces exerted on a terrestrial structure caused by a collision-induced tsunami. Conventionally, assessing these forces relies on the inundation depth of the colliding tsunami passing without the presence of the terrestrial structure. However, it is essential to consider the inundation depth and incident fluid velocity, as both significantly influence the resulting tsunami forces. In this research, ANSYS Fluent 17.2 is employed to simulate excitation sources using a Defined Function (UDF) code within a C++ framework. The dynamic meshing technique is adopted to replicate the interactions between the bore pressure of the tsunami and an idealised vertical wall structure across three distinct water levels. Computational Fluid Dynamics (CFD) modelling demonstrates the proposed methodology's capability to offer precise impact pressure distributions concerning geographical and temporal aspects. The findings reveal specific instances: at a water depth of 10 m, the maximum Froude number is attained at 3.5 and 6.9 seconds, corresponding to a maximum pressure value of 3.9x105 Pa at 3.85 seconds for a water flow velocity of 20 m/sec. Similarly, for a water depth of 12 m, the most significant Froude number is observed at 3.95 and 6.9 seconds, with a peak pressure value of 1.8x105 Pa at 4.6 seconds, associated with a water flow velocity of 15 m/s. Additionally, at a water depth of 14 m, the maximum Froude number is reached at 4.95 and 7.1 seconds, accompanied by a maximum pressure value of 7.4x104 Pa at 4.85 seconds for a water flow velocity of 10 m/s.

1. Introduction

Wind energy is available, sustainable, environmentally friendly, and cost-effective by Khader and Nada [1]; and Thomai *et al.,* [2]. Tremendous wind energy is used in open spaces such as remote or offshore countryside using large-scale Horizontal Axis Wind Turbines by Manganhar *et al.,* [3]. Due to fast and cost-effective production costs, many aerodynamic theories were implemented on Vertical Axis Wind Turbine type by Ismail *et al.,* [4]; and C M *et al.,* [5]. Raynaud's effect on the slotted Savonius turbine. Slotted blades reduce airflow, hitting convex blades through gaps, reducing

* *Corresponding author.*
E-mail address: *imam.muzaki@ubpkarawang.ac.id (Imam Muzaki)*

https://doi.org/10.37934/cfdl.16.5.121134

negative torque, and increasing turbine power coefficient by Tjahjana *et al.,* [6]. Savonius turbines are simpler, self-starting, have low-speed wind processes, and have low noise by Siddiqui *et al.,* [7]; and Ismail *et al.,* [8].

Yuwono *et al.,* [9] analyzed the Improving the performance of the Savonius wind turbine by installation of a circular cylinder upstream of the returning turbine blade. Savonius rotor aerodynamic performance has been improved continuously. It focuses on the design modification in which the evaluation is conducted through numerical evaluation and experimental tests. The proposed design shows an overall improvement of 16.7% to 18%. Thus, it has a suitable aerodynamic performance by Pranta *et al.,* [10].

Al-Ghriybah *et al.,* [11] and Suyitno *et al.,* [12] studied the effect of the position of the inner blade on the performance of the Savonius rotor, whose torque coefficient increased significantly after the Savonius rotor was modified with the inner blade. According to the numerical analysis of Eshagh *et al.,* [13]; and Tahani *et al.,* [14], Discharge flow capability and severe adverse impacts on turbine performance for optimal design configurations. The results show that the porous deflector produces higher positive torque. Assessment of turbine performance and modifying the turbine system by adding a nozzle. Elbatran *et al.,* [15]; Prabowo and Prabowoputra [16]. Studied the performance of Savonius water turbine duct nozzles, compared with conventional Savonius turbines, which, by implementing a duct nozzle, has significantly improved the performance of the Savonius turbine.

The size of the air ejector and the Savonius turbine model have a unique role in the power coefficient. The lack of research specifically addresses the influence of air ejectors and savonius turbine models makes these two things need to be analyzed further. This research focuses in depth on the simulation of adding air ejectors Model 1: 450 mm x 450 mm, Model 2: 500 mm x 500 mm, Model 3: 550 mm x 550 mm, to savonius wind turbines using Computational Fluid Dynamic software to examine how air ejector dimensions affect savonius rotor performance.

2. Methodology

2.1 CFD Modeling

The design of the air ejector is made with a length of 200 mm, and the dimensions of the inlet at the end of the object are three models wide, namely 450 mm x 450 mm, 500 mm x 500 mm, 550 mm x 550 mm, while the inlet in the narrow hole of 375 mm x 375 mm is designed to maximize wind speed. Figure 1 shows the design of the planned air ejector in this study.

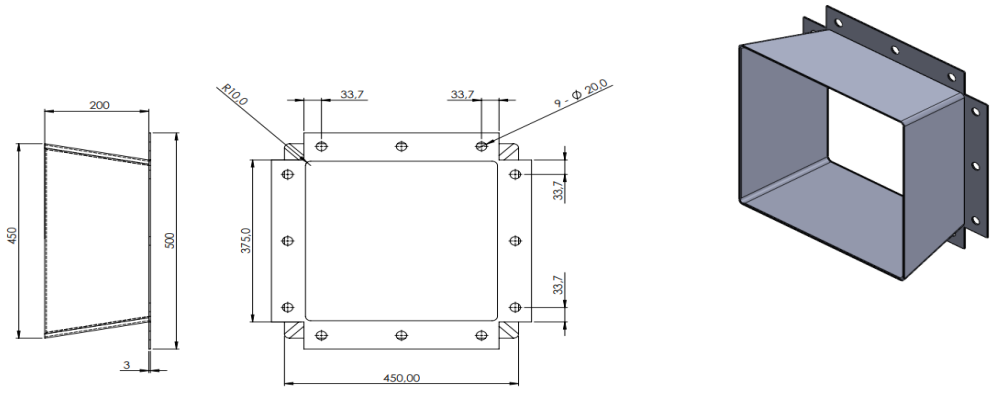

(a) (b) (c)

Fig. 1. Schematic design of the air ejector, (a) side view, (b) front view, (c) 3D design

The design of the Savonius wind turbine with the addition of two blades on the inside in both semicircular blades already exists in conventional configurations with different dimensions of the turbine height. Design modelled using solidwork software by Al-Ghriybah *et al.,* [17]. Figure 2, Figure 3, and Figure 4 a Savonius wind turbine design and geometry 1-stage and 2-stage planned in this study.

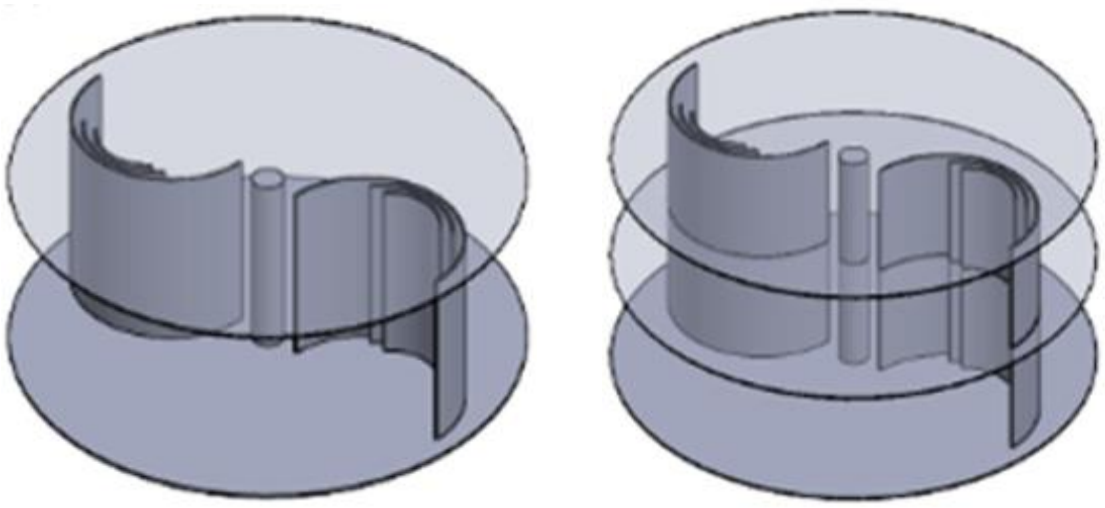

(a) (b)

Fig. 2. Savonius turbine design (a) 1-stage, (b) 2- stage

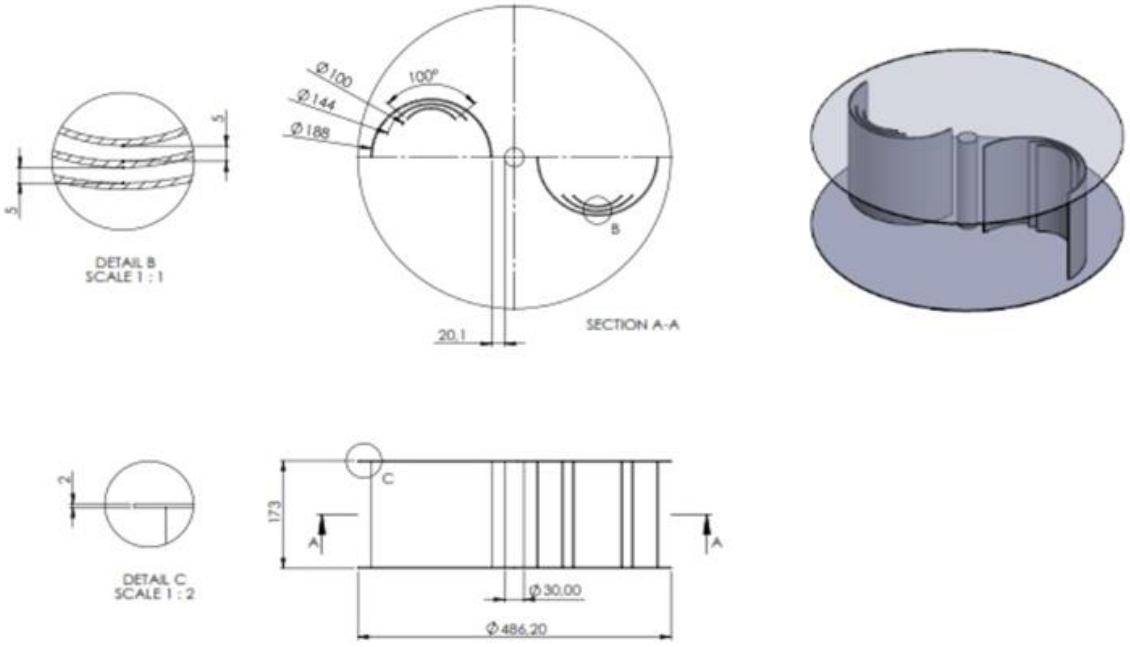

Fig. 3. Design and geometry of wind turbine Savonius 1-stage

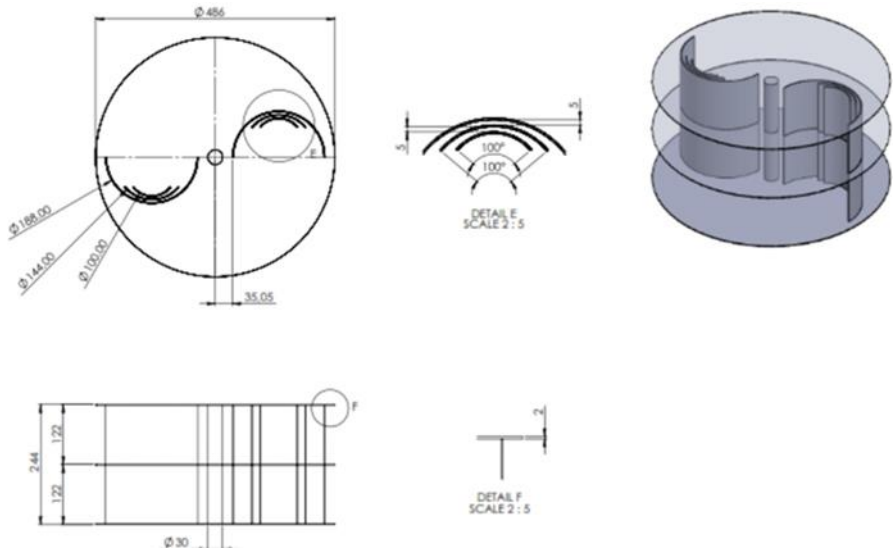

Fig. 4. Design and geometry of wind turbine Savonius 2-stage

After the design of the air ejector and the Savonius wind turbine model are determined, the next step is to determine the input parameters so that the value of each part is determined based on references used in various journals for the simulation process. Table 1 provides dimension values for the simulation process.

Table 1
Dimension values for the simulation process

Description	value
Air ejector length	200 mm
Output channel	375 mm x 375 mm
Inner corner of the blade	100o
Number of inner blades	2
The distance between the inner blades	5 mm
Turbine diameter (De)	1100 mm
Rotor diameter (D)	442 mm
Diameter of the main blade (d)	188 mm
The first diameter of the inner blade (d1)	144 mm
Diameter of the two inner blades (d2)	100 mm
The thickness of all blades (t)	2 mm

Computational Fluid Dynamic (CFD) is used to transform fluid dynamics equations in the form of integrals and derivatives into discretized algebraic structures. The governing equations in fluid dynamics are Eq. (1), explaining continuity in differential form, and Eq. (2), regarding momentum. Eq. (3) regarding Energy in the form of internal Energy.

$$\frac{\partial \rho}{\partial t} + \rho \vec{\nabla} \cdot \vec{V} = 0 \tag{1}$$

$$\frac{\partial (\rho u)}{\partial t} + \vec{\nabla} \cdot \left(\rho u \vec{V}\right) = -\frac{\partial p}{\partial x} + \frac{\partial \tau_{xx}}{\partial x} + \frac{\partial \tau_{yx}}{\partial y} + \frac{\partial \tau_{zx}}{\partial z} + \rho f_x \tag{2}$$

$$\frac{\partial}{\partial t}\left[\rho\left(e + \frac{V^2}{2}\right)\right] + \vec{\nabla} \cdot \left[\rho\left(e + \frac{V^2}{2}\right)\vec{V}\right] = \rho \dot{q} - \frac{\partial (\rho p)}{\partial x} - \frac{\partial (vp)}{\partial y} - \frac{\partial (wp)}{\partial z} + \rho \vec{f} \cdot \vec{V} \tag{3}$$

The solution of a partial differential analytical equation results in a continuously closed form dependent variable expression across domains. In contrast, the resolution of a numerical equation can only assign a value to a discrete point in the domain, called a grid point by Saad *et al.,* [18]. Simulation is aimed at determining the best power coefficient of each variable tested. Table 2 is a variable model for simulation.

Table 2
Variable model for simulation

Description	value
Air ejector input line	Model 1: 450 mm x 450 mm Model 2: 500 mm x 500 mm Model 3: 550 mm x 550 mm
Rotor height 1- stage	173 mm
Rotor height 2-stage	122 mm

To improve the performance of Savonius wind turbines, modifications were made to the wind intake system by adding an air ejector. Computer-aided design (CAD) models are prepared for both configurations. The transient simulation will be performed on a 3D model of the rotor so that the CAD model consists of two rotating domains connected; one represents a rotating domain containing the rotor geometry, and the other is a stationary domain that represents a fully enveloping environment of the rotating domain indicated Figure 5 is a detailed limitation of the CAD model.

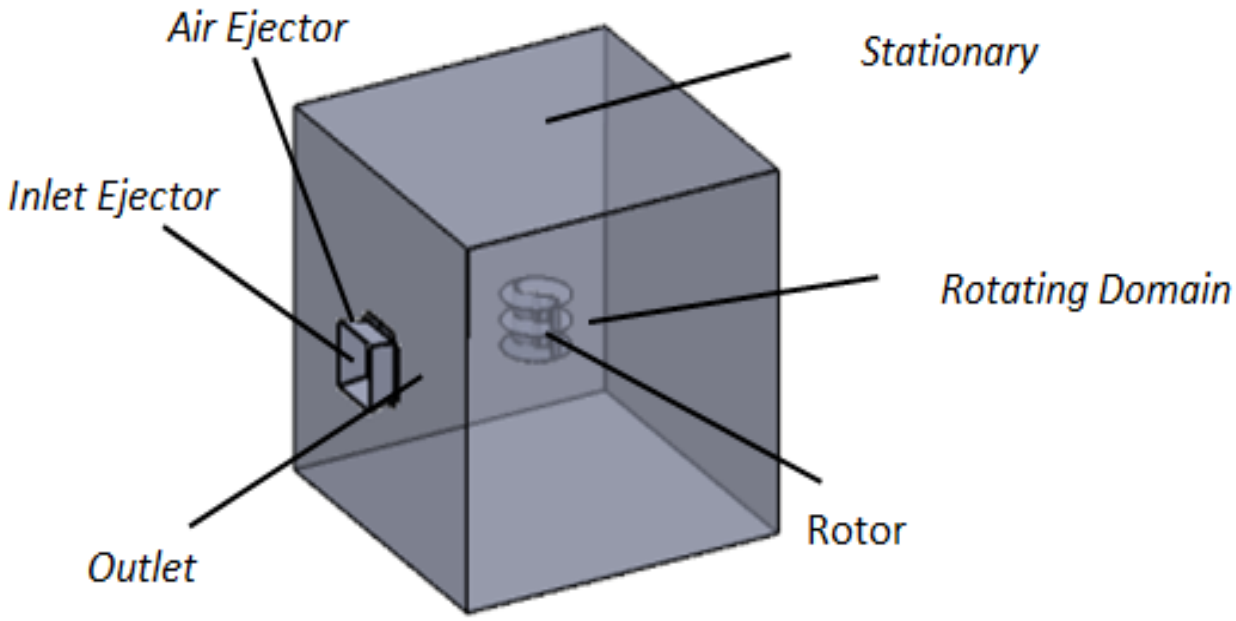

Fig. 5. CAD model limit details

2.2 Model Domain and Meshing

Computational settings are used in simulations to obtain the distribution of wind flow on wind turbines by Bai *et al.,* [19]. Turbulent: K-omega SST k-omega models are used for their advantages in simulating adverse pressure gradient flows and narrow gaps such as piping. SST modifications accommodate areas with free streams, such as areas far from the wall. Cell Zone Condition for the

rotary domain is given frame motion to represent the rotating motion in the turbine with the input of angular velocity values. In contrast, for the cavity domain it is a silent domain. Solution Initialization is the initial reference of the iteration process, where the closer the initial consideration is to the expected solution, the more stable the iteration process will be, and concurrent conditions will be achieved faster. The method used is standard initialization because it chooses one inlet direction to adjust the initial value to the inlet. Settings are not mentioned using existing default settings.

The next stage is the formation of a mesh against the computational domain by Ferrari *et al.,* [20]. Meshing or discretization in the Savonius turbine CFD simulation uses the meshing linear method because it captures complex and detailed geometries in wind turbines by Krysinski *et al.,* [21]. Figure 6 displays the overall results of selecting linear meshing and meshing around the turbine.

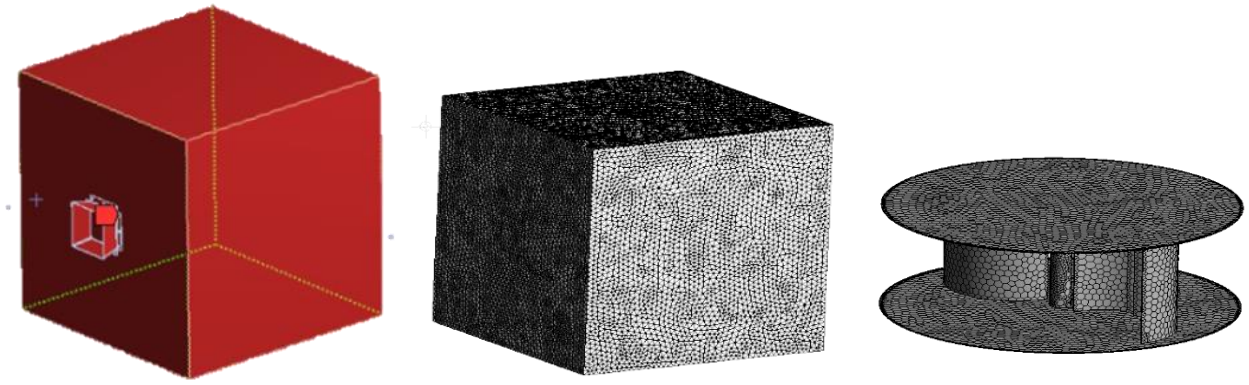

(a) (b) (c)

Fig. 6. Result (a) Simulation domain, (b) overall linear meshing, (c) meshing around the turbine

2.3 Boundary Conditions and Flow Solver

The input used in the boundary conditions is the velocity-inlet at the inlet, defined as the velocity inlet with a speed of 2 m/s, 3 m/s, 4 m/s and 5 m/s. The walls on surface walls are defined as walls with no slip conditions representing friction between the fluid and the wall. The outlet section's pressure outlet means the flow's egress. The boundary condition at the outlet is defined as the pressure outlet. The computational domain's upper and lower edges are considered boundary conditions of symmetry. The SIMPLE algorithm is used for the solution method by Alipour *et al.,* [22]

3. Results and Discussion

3.1 Model Validation

Before the simulation starts, there is one step that must be completed, which is to compare the simulation results with the results from previous studies. This ensures that the simulation methods used are reliable and accurate enough to be used for the remainder of the simulation. As a result, the validation process is carried out by transferring the specific settings from the previous study to the current simulation settings to obtain the most comparable results. The power coefficients were evaluated for this study using the simulation settings of earlier studies, and the results were compared with those from ref by Elbatran *et al.,* [15].

In Figure 7, the value of the power coefficient is plotted against the Tip Speed Ratio (TSR), which corresponds to the results of the current study with the addition of an air ejector and the results of previous studies using a nozzle on a Savonius wind turbine. The graph shows that the trend between the current and previous study results shows an increasing trend evaluated on average around 14%.

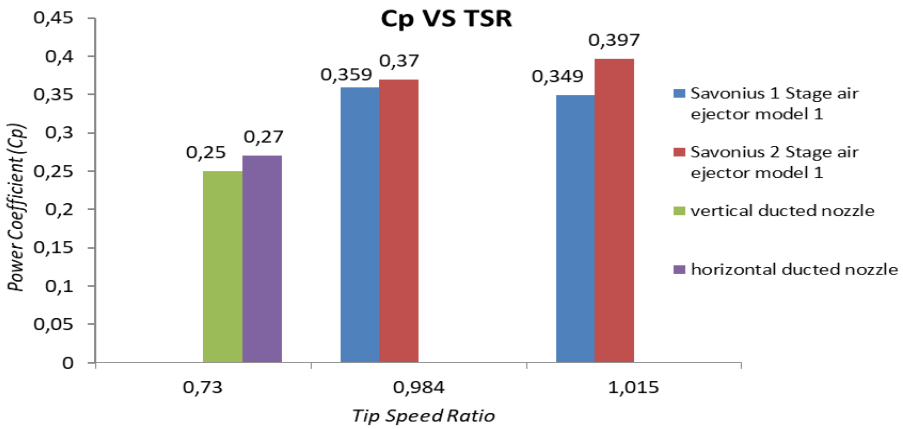

Fig. 7. The comparison between current and previous results

3.2 Simulation Result

The rotating motion of the rotor causes the fluid surrounding the rotor to also rotate to a certain extent at the turbine blade turning. The fluid entering the interior of the turbine blades is also directed tangentially when the rotating fluid motion on the opposite side of the outer blade inhibits the turbine blade turning. Because of this case, the fluid deflection at the return vane enters the periphery of the rotating domain, resulting in a high fluid flow velocity. Figure 8 displays the flow velocity distribution in the rotating domain of the 1-stage and 2-stage Savonius wind turbines. It is known that the top speed of turbines 1 and 2 is 18 m/s, which is shown when the angle is 0°. The interior of the turbine blades has an average flow velocity of 4 m/s.

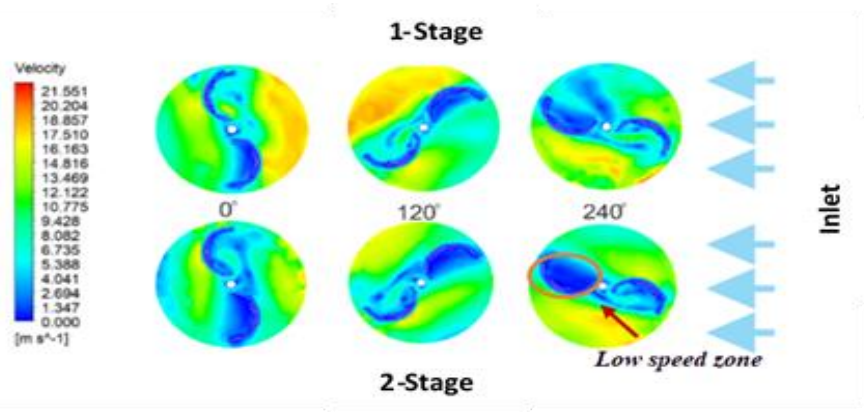

Fig. 8. Distribution of flow velocity in the rotating domain of level 1 and 2 wind turbines

In the 2-stage Savonius wind turbine, the interior blades are more evenly distributed than in the 1-stage Savonius wind turbine. Figure 9 displays the distribution of forces on the 1st and 2nd stage rotors. The average thrust of a 2-stage Savonius wind turbine at an angle 0° of 0.026 N and at an angle 120° by 0.020 N smaller than the Savonius 1-stage wind turbine at an angle 0° of 0.033 N and at an angle 120° of 0.026 N. However, in addition to the increased thrust, the force that inhibits the turbine blades also increases with the most significant force of 0.072 N, owned mainly by the return blades outside the 1-story Savonius wind turbine.

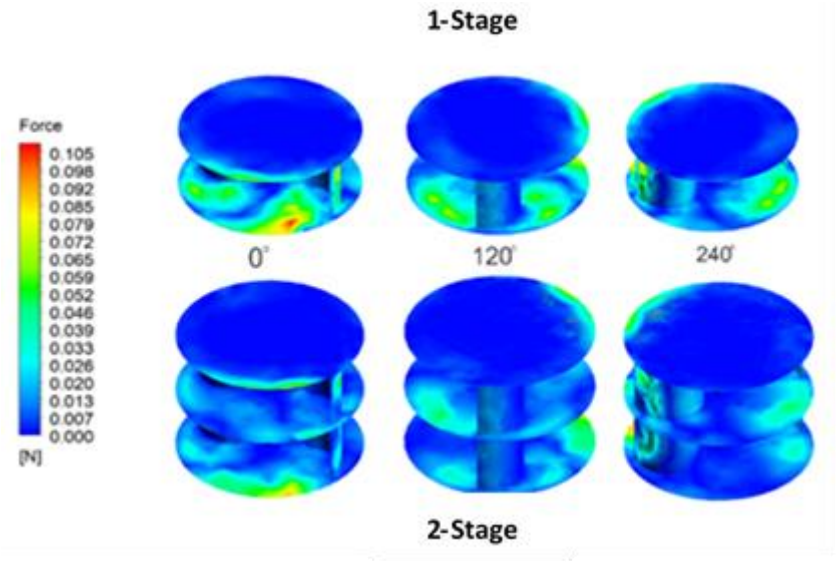

Fig. 9. Force distribution on 1 stage and 2 stage rotor

3.3 Performance Analysis of Simulation Results

Figure 10 (a) illustrates the performance of the power coefficient with the TSR air ejector model 1. The most significant power coefficient value for the Savonius 2-level wind turbine model 1 air ejector at a TSR of 1.015 is 0.397, while the most enormous power coefficient value for the Savonius 1-level vertical axis wind turbine is 0.359 at a TSR of 0.984. The power coefficient performance with TSR air ejector Model 2 is shown in Figure 10 (b), with the immense power coefficient value for the Savonius 2 wind turbine model 2 air ejector level at TSR 0.799 of 0.395 while the most significant power coefficient value for the vertical axis Savonius 1 level wind turbine is 0.304 at TSR of 0.799. The performance of the power coefficient with the TSR air ejector model 3 is shown in Figure 10 (c), with the largest power coefficient value for the Savonius 2-level wind turbine model 3 air ejector at TSR 0.661 of 0.345 while the most significant power coefficient value for the Savonius 1 level vertical axis wind turbine is 0.301 at TSR 0.661.

Comparison of Savonius 2 stage vertical axis wind turbine has a higher power coefficient performance on air ejector models 1 and 2 than Savonius 1 stage wind turbine. While the air ejector model 3 vertical axis wind turbine Savonius 1 level is obtained at TSR 0.661, the power coefficient (Cp) is 0.301, at TSR 0.659, the power coefficient is 0.235, and for the Savonius 2 vertical axis wind turbine, the power coefficient level is 0.187 at TSR 0.661 while at TSR 0.659 power coefficient is 0.129. At TSR 0.661 and 0.659, the best power coefficient performance is in the Savonius 1 vertical axis wind turbine, which is higher than the Savonius 2 vertical axis wind turbine.

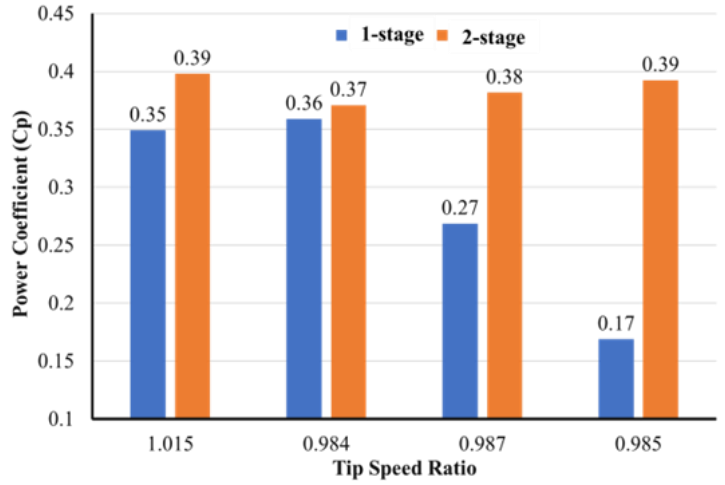

(a)

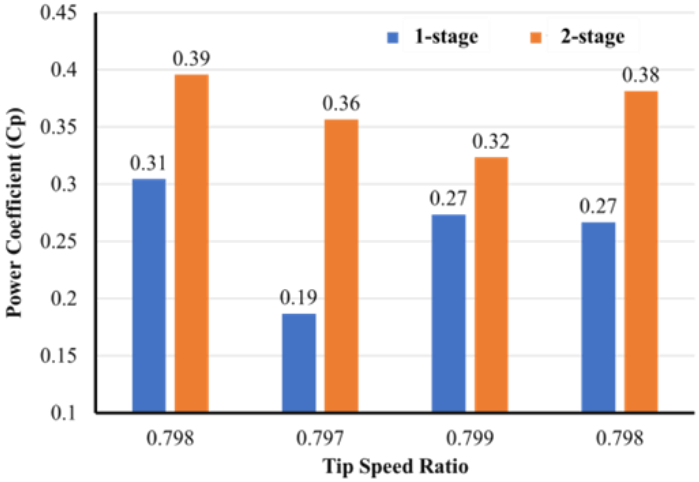

(b)

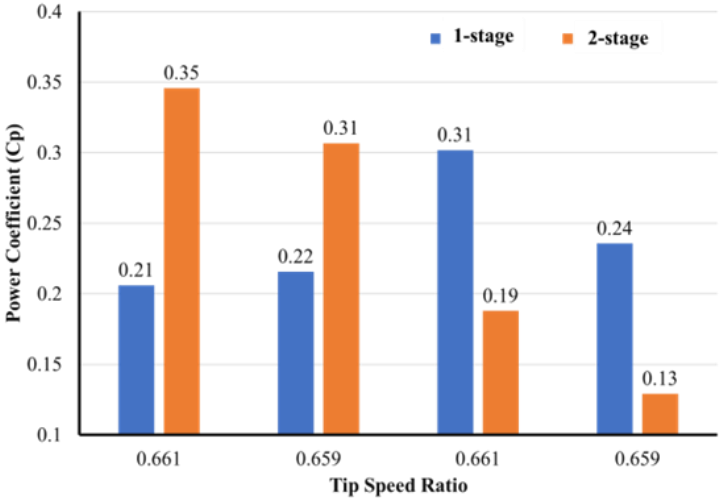

(c)

Fig. 10. Power coefficient performance vs TSR air ejector (a) model 1, (b) model 2, (c) model 3

Based on Figure 11 (a), the torque coefficient performance with TSR air ejector model 1 shows that the most considerable torque coefficient value for the Savonius 2 wind turbine model 1 air ejector level at TSR 0.985 is 0.773 while the most considerable torque coefficient value for Savonius

1 level vertical axis wind turbine is 0.668 at TSR 1.015. The torque coefficient performance with TSR air ejector Model 2 is shown in Figure 11 (b) with the enormous torque coefficient value for the Savonius 2 wind turbine model 2 level air ejector at TSR 0.799 of 0.962 while the most significant torque coefficient value for the vertical axis Savonius 1 level wind turbine is 0.740 at TSR 0.799.

The performance of the torque coefficient with the TSR air ejector model 3 is shown in Figure 11 (c) with the largest torque coefficient value for the Savonius 2 level air ejector wind turbine model 3 at TSR 0.661 of 1.017 while the largest torque coefficient value for the Savonius 1 level vertical axis wind turbine is 0.887 at TSR 0.661.

For the air ejector model 3 of the Savonius 1 vertical axis wind turbine, the torque coefficient of TSR is 0.661 (Cq) of 0.887, the TSR of 0.659 is the torque coefficient of 0.694, and for the Savonius 2 vertical axis wind turbine the torque coefficient is 0.552 at the TSR of 0.661. TSR 0.659 torque coefficient is 0.381. At TSR of 0.661 and 0.659, the best torque coefficient performance is in the Savonius 1 vertical axis wind turbine, which is higher than the Savonius 2 vertical axis wind turbine.

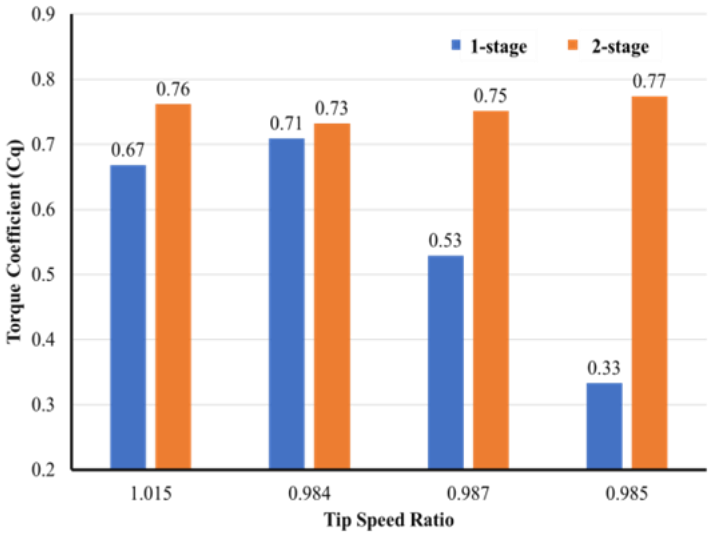

(a)

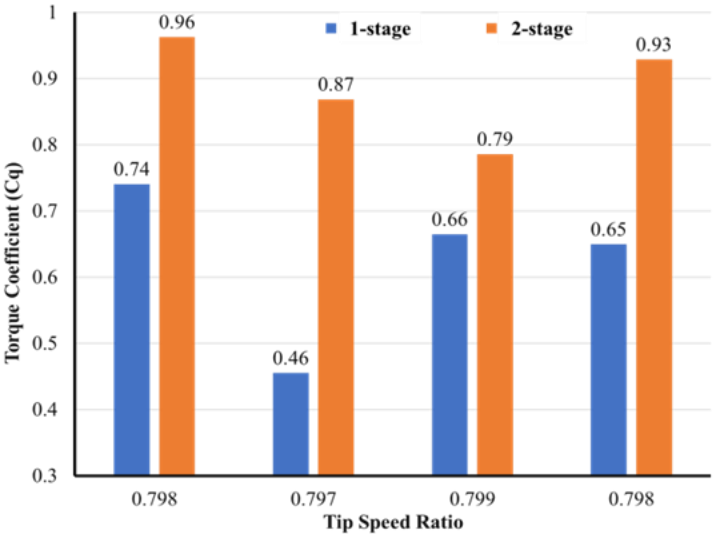

(b)

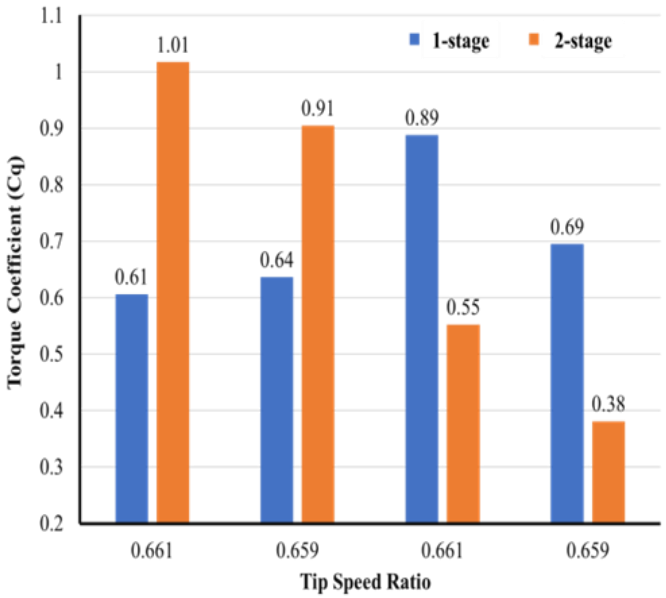

(c)

Fig. 11. Torque coefficient performance vs TSR air ejector model (a) model 1, (b) model 2, (c) model 3

Figure 12 (a) shows the transient torque to the angle of rotation from the air ejector model 1. The peak torque for 1 stage reaches 0.06 Nm at the angle of rotation 90°, while for 2stages, it reaches 0.12 Nm at angle of rotation 60°. Based on Figure 12 (b), transient torque to angle of rotation results of air ejector model 2 that the peak torque for 1. Stage reaches 0.06 Nm at angle of rotation 90° while for 2 levels it reaches 0.21 Mm at angle of rotation 130°. Figure 12 (c) shows the transient torque to the angle of rotation simulation of the model 3 air ejector that the peak torque value for the Savonius 1 stage wind turbine reaches 0.08 Nm at the angle of rotation 80° while for the 2. Stage Savonius wind turbine at an angle of rotation 80° went a value of 0.17 Nm. These data show that the torsional oscillation experienced by the Savonius type 2 level vertical axis wind turbine is higher than 1 level.

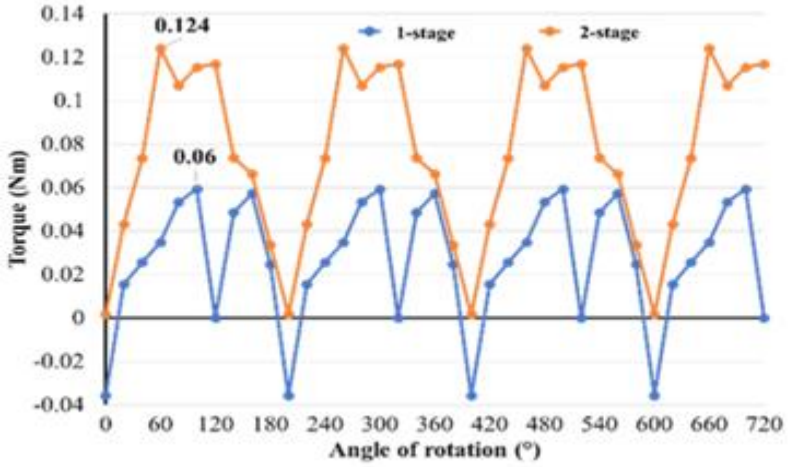

(a)

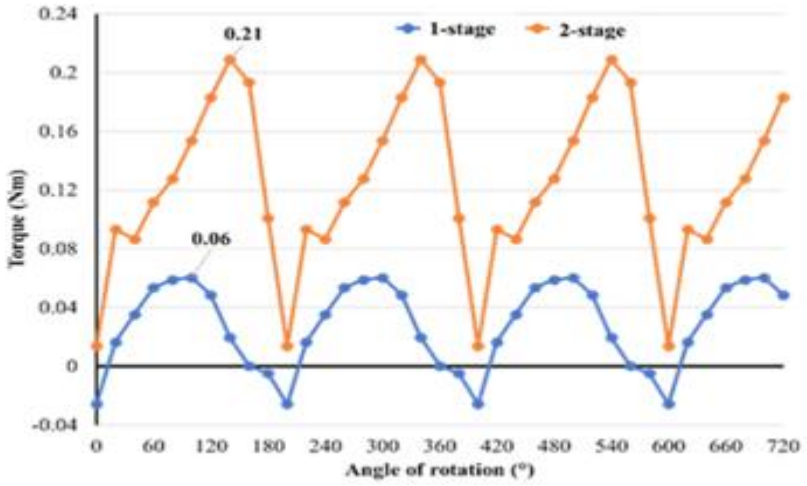

(b)

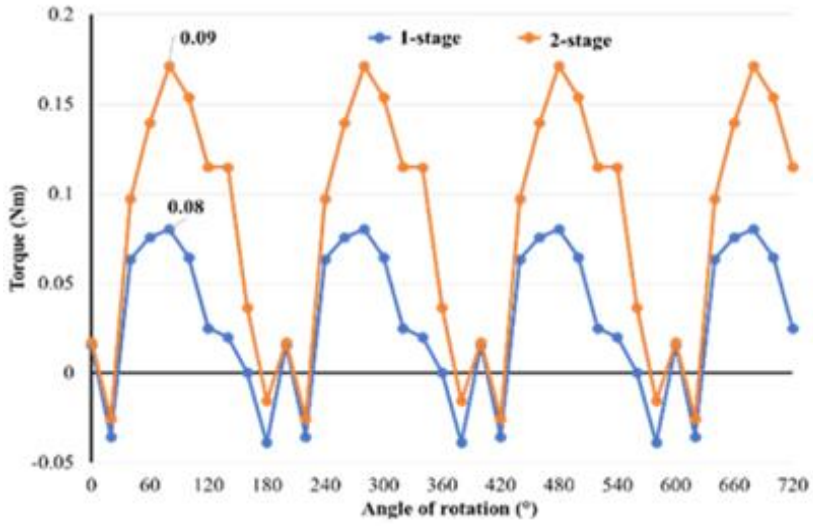

(c)

Fig. 12. Transient torque to angle of rotation air ejector (a) model 1, (b) model 2, (c) model 3

4. Conclusion

Provide results that the air ejector model 2 and the Savonius 2 stage wind turbine model have the best performance compared to the air ejector model 2 and the Savonius 1 stage wind turbine model. The best model is shown by the air ejector model 2 of the Savonius 2-level wind turbine, where this model can achieve performance at TSR 0.798 with a power coefficient value of 0.381. This result can reference the increase in 4 m/s wind speed. The recommendation for the subsequent research is to conduct experiments experimentally by paying attention to the same variables in this simulation.

Acknowledgement
The authors acknowledge and appreciate the cooperation of Universitas Pancasila – Indonesia for their assistance in this research, and any grant did not fund this research.

References

[1] Khader, Khaled M., and Omayma A. Nada. "Using crank-crank mechanism to reorient flat blades of vertical wind turbine for improving its performance." *Alexandria Engineering Journal* 59, no. 6 (2020): 4147-4157. https://doi.org/10.1016/j.aej.2020.07.020.

[2] Thomai, Micha Premkumar, Seralathan Sivamani, and Hariram Venkatesan. "Dataset on the measurement of power in the hybrid vertical axis wind turbine in natural wind." *Data in Brief* 31 (2020): 105922. https://doi.org/10.1016/j.dib.2020.105922.

[3] Manganhar, Abdul Latif, Altaf Hussain Rajpar, Muhammad Ramzan Luhur, Saleem Raza Samo, and Mehtab Manganhar. "Performance analysis of a savonius vertical axis wind turbine integrated with wind accelerating and guiding rotor house." *Renewable Energy* 136 (2019): 512-520. https://doi.org/10.1016/j.renene.2018.12.124.

[4] Ismail, Ismail, Reza Abdu Rahman, Gunady Haryanto, and Erlanda Augupta Pane. "The optimal pitch distance for maximizing the power ratio for savonius turbine on inline configuration." *International Journal of Renewable Energy Research (IJRER)* 11, no. 2 (2021): 595-599.https://doi.org/10.20508/ijrer.v11i2.11862.g8181.

[5] Shashikumar, C. M., Ramesh Honnasiddaiah, Vijaykumar Hindasageri, and Vasudeva Madav. "Studies on application of vertical axis hydro turbine for sustainable power generation in irrigation channels with different bed slopes." *Renewable energy* 163 (2021): 845-857. https://doi.org/10.1016/j.renene.2020.09.015.

[6] Tjahjana, Dominicus Danardono Dwi Prija, Zainal Arifin, Suyitno Suyitno, Wibawa Endra Juwana, Aditya Rio Prabowo, and Catur Harsito. "Experimental study of the effect of slotted blades on the Savonius wind turbine performance." *Theoretical and Applied Mechanics Letters* 11, no. 3 (2021): 100249. https://doi.org/10.1016/j.taml.2021.100249.

[7] Siddiqui, M. Salman, Muhammad Hamza Khalid, Rizwan Zahoor, Fahad Sarfraz Butt, Muhammed Saeed, and Abdul Waheed Badar. "A numerical investigation to analyze effect of turbulence and ground clearance on the performance of a roof top vertical–axis wind turbine." *Renewable Energy* 164 (2021): 978-989. https://doi.org/10.1016/j.renene.2020.10.022.

[8] Ismail, I., E. A. Pane, G. Haryanto, T. Okviyanto, and R. A. Rahman. "A Better Approach for Modified Bach-Type Savonius Turbine Optimization." *Int Rev Aerosp Eng* 14 (2021): 159. https://doi.org/10.15866/irease.v14i3.20612.

[9] Yuwono, Triyogi, Gunawan Sakti, Fatowil Nur Aulia, and Adi Chandra Wijaya. "Improving the performance of Savonius wind turbine by installation of a circular cylinder upstream of returning turbine blade." *Alexandria Engineering Journal* 59, no. 6 (2020): 4923-4932. https://doi.org/10.1016/j.aej.2020.09.009.

[10] Pranta, M. H., M. S. Rabbi, and M. M. Roshid. "A computational study on the aerodynamic performance of modified savonius wind turbine." *Results in Engineering* 10 (2021): 100237. https://doi.org/10.1016/j.rineng.2021.100237.

[11] Al-Ghriybah, Mohanad, Mohd Fadhli Zulkafli, Djamal Hissein Didane, and Sofian Mohd. "The effect of inner blade position on the performance of the Savonius rotor." *Sustainable Energy Technologies and Assessments* 36 (2019): 100534. https://doi.org/10.1016/j.seta.2019.100534.

[12] Suyitno, BUDHI MULIAWAN, REZA ABDU Rahman, I. Ismail, and E. A. Pane. "Increasing the Energy Density and Power Ratio of a Staggered VAWT Wind Farm by using The Rotor's Diameter as a Reference." *WSEAS Transactions on Fluid Mechanics* 17 (2022): 60-7. https://doi.org/10.37394/232013.2022.17.6.

[13] Nimvari, Majid Eshagh, Hossein Fatahian, and Esmaeel Fatahian. "Performance improvement of a Savonius vertical axis wind turbine using a porous deflector." *Energy Conversion and Management* 220 (2020): 113062. https://doi.org/10.1016/j.enconman.2020.113062.

[14] Tahani, Mojtaba, Ali Rabbani, Alibakhsh Kasaeian, Mehdi Mehrpooya, and Mojtaba Mirhosseini. "Design and numerical investigation of Savonius wind turbine with discharge flow directing capability." *Energy* 130 (2017): 327-338. https://doi.org/10.1016/j.energy.2017.04.125.

[15] Elbatran, A. H., Yasser M. Ahmed, and Ahmed S. Shehata. "Performance study of ducted nozzle Savonius water turbine, comparison with conventional Savonius turbine." *Energy* 134 (2017): 566-584. https://doi.org/10.1016/j.energy.2017.06.041.

[16] Prabowo, Aditya Rio, and Dandun Mahesa Prabowoputra. "Investigation on Savonius turbine technology as harvesting instrument of non-fossil energy: Technical development and potential implementation." *Theoretical and Applied Mechanics Letters* 10, no. 4 (2020): 262-269. https://doi.org/10.1016/j.taml.2020.01.034.

[17] Al-Ghriybah, Mohanad, Mohd Fadhli Zulkafli, Djamal Hissein Didane, and Sofian Mohd. "The effect of spacing between inner blades on the performance of the Savonius wind turbine." *Sustainable Energy Technologies and Assessments* 43 (2021): 100988. https://doi.org/10.1016/j.seta.2020.100988.

[18] Saad, Ahmed S., Ibrahim I. El-Sharkawy, Shinichi Ookawara, and Mahmoud Ahmed. "Performance enhancement of twisted-bladed Savonius vertical axis wind turbines." *Energy Conversion and Management* 209 (2020): 112673. https://doi.org/10.1016/j.enconman.2020.112673.

[19] Bai, H. L., Chun Man Chan, X. M. Zhu, and K. M. Li. "A numerical study on the performance of a Savonius-type

vertical-axis wind turbine in a confined long channel." *Renewable Energy* 139 (2019): 102-109. https://doi.org/10.1016/j.renene.2019.02.044.

[20] Ferrari, G., D. Federici, Paolo Schito, Fabio Inzoli, and Riccardo Mereu. "CFD study of Savonius wind turbine: 3D model validation and parametric analysis." *Renewable energy* 105 (2017): 722-734.https://doi.org/10.1016/j.renene.2016.12.077.

[21] Krysinski, Tomasz, Zbigniew Bulinski, and Andrzej J. Nowak. 2019. Numerical Modelling of a Savonius Wind Turbine Using the URANS Turbulence Modelling Approach. Springer Tracts in Mechanical Engineering. Springer International Publishing. https://doi.org/10.1007/978-3-030-11887-7_10.

[22] Alipour, Ramin, Roozbeh Alipour, Farhad Fardian, Seyed Saeid Rahimian Koloor, and Michal Petrů. "Performance improvement of a new proposed Savonius hydrokinetic turbine: a numerical investigation." *Energy Reports* 6 (2020): 3051-3066. https://doi.org/10.1016/j.egyr.2020.10.072.